Mat. Res. Soc. Symp. Proc. Vol. 691 © 2002 Materials Research Society

Synthesis and Properties of Lead Selenide Nanocrystal Solids

Feng Chen[a], Kevin L. Stokes[a], Weilie Zhou[a], Jiye Fang[a] and Christopher B. Murray[b]
[a]Advanced Material Research Institute, University of New Orleans, New Orleans, LA 70148, USA
[b]IBM T.J. Watson Research Center, Yorktown Heights, NY 10598, USA

ABSTRACT

We present results of our investigation of the synthesis, structural properties and electrical transport properties of lead selenide (PbSe) nanoparticle-derived solids. Stable colloidal solutions containing crystalline PbSe particles with sizes on the order of 5–10 nm were synthesized using an organometallic lyothermal growth method in high-temperature organic solvents (100∼200 °C). The nanoparticle powders have been characterized by X-ray scattering (WAXS/SAXS), electron microscopy and optical absorption. Thin films were formed by controlled precipitation of the nanoparticles from solution onto insulating substrates. Electrical resistance (R) and Seebeck coefficient (S) for conductive PbSe films from different annealing conditions were studied and compared. We were able to obtain conductive PbSe films from colloids by low temperature annealing which did not disturb the nanoparticle self-assembly.

INTRODUCTION

Bulk PbSe is one of the promising materials for the thermoelectric cooling and power generating devices [1]. Nanoparticles can potentially improve the thermoelectric properties over bulk by increasing the Seebeck coefficient due to the altered electronic density of states or making use of a compositionally modulated material that would block phonons while transmitting electrons [2–5]. Nanoparticles prepared by colloidal method were used for fabricating self-assembled films [6]. However, the organic capping species between the nanoparticles need to be removed without destroying the nanoparticle arrangement. We report here the synthesis, structural properties and electrical transport properties of PbSe thin films.

EXPERIMENTAL DETAILS

The colloidal PbSe nanocrystallites were synthesized using a high temperature co-precipitation approach in organic solution [7, 8]. Typically, lead acetate was dissolved in diphenyl ether along with oleic acid (stabilizing agent). The mixture was heated up to 180 °C under flowing argon with constant stirring, then trioctylphosphine (TOP) with pre-dissolved Se metal (1M) was injected in using a syringe, and the system was maintained at 180 °C for 10 minutes under argon environment. The resulting PbSe colloid was then cooled down to room temperature and subsequently precipitated by adding a polar alcohol solvent and centrifugation. The particles were redispersed in a proper solvent such as hexane, octane or trichloro-triflouroethane. The particle size of PbSe ranged from ∼5 nm to 10 nm. To further narrow the size distribution, a size-selection treatment was performed using the solvent-nonsolvent pair of hexane and ethanol [8]. The resulting

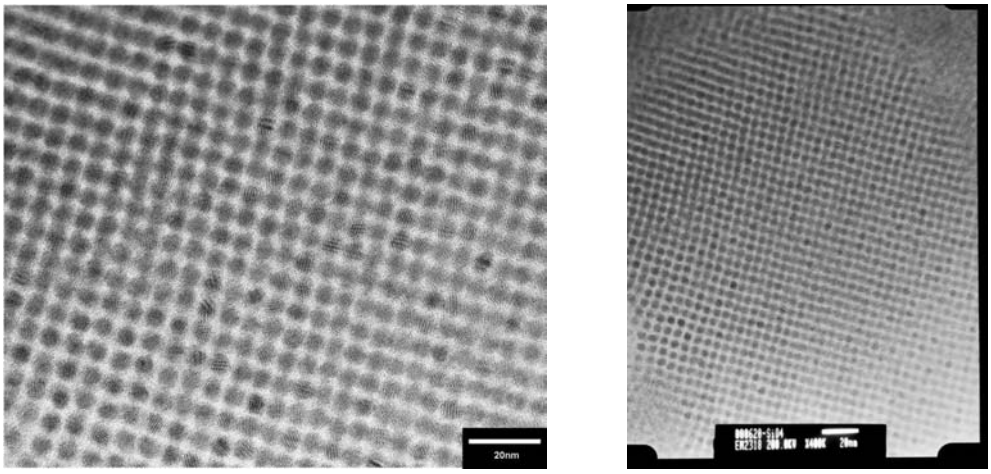

Figure 1: Left: self-assembled 6 nm PbSe nanoparticles. Right: 0.3×0.4 μm area of self-assembled nanoparticles.

monodispersed PbSe suspension in hexane was dropped onto a TEM (transmission electron microscope) grid and dried. By directly measuring the particle size from the TEM image and compiling the statistics on ∼100 particles, the particle diameters were determined to be 6.0 nm with less than 10% size distribution. As a result, we were able to obtain good self-assembly of PbSe in the area of at least 0.3×0.4 μm (Figure 1).

UV-Vis-NIR optical absorption was measured by dissolving PbSe nanoparticles in $C_2Cl_3F_3$ to form a stable colloidal suspension. This particular solvent was used because it does not have any C–H absorption peaks in the near infrared region of the optical spectrum.

The PbSe films were obtained by a controlled evaporation/precipitation method. We used different solvents mentioned above to get differing evaporation rates. A small amount of higher boiling point polar solvent was added so that the particles fall out of solution *before* all the solvents evaporate [6]. The organic materials between the particles were finally removed by annealing at high temperature from 200 to 500 °C.

The resistance was measured using dc four-probe method. The Seebeck coefficient was measured using a very low frequency ac two-heater method [9]. Two surface mount resistors were driven by sinusoid currents that differ in phase by $\pi/2$. Two pairs of T-type thermocouple were attached to the sample directly using EPO-TEC H20E silver epoxy and three independent signals were measured simultaneously to solve for the base temperature, temperature gradient and the Seebeck coefficient. The copper leads of the T-type thermocouple were calibrated relative to Pb using data from Roberts [10].

The resistance across the film we measured was typically ∼100 kΩ at 100 K. This contributed considerable amount of noise to the signals. We adopted some improvement to the method mentioned in our previous setup [9]. Basically, among four electrical leads, there are 6 paired combinations of the leads and any 3 of them are independent. A different choice of these 3 pairs of leads is more suitable for highly resistive samples. The details are mentioned elsewhere [11].

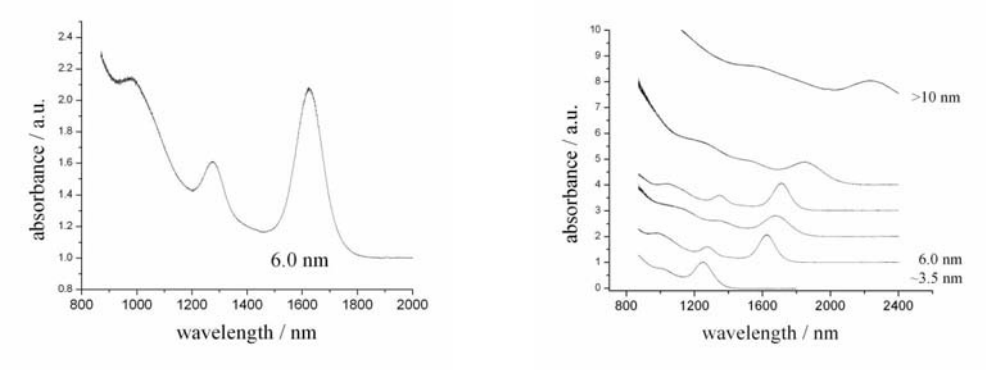

Figure 2: UV-Vis-NIR optical absorption of PbSe colloids. Left: a typical curve for 6.0 nm particles showing sharp absorption peak. Right: the absorption peak shifting to shorter wavelength with decreasing particle size.

RESULTS AND DISCUSSION

Different sized particles were obtained by adjusting the reaction temperature (T), reaction time (t) and relative TOP concentration and verified by TEM and UV-Vis-NIR optical absorption. The optical absorption results are shown in Figure 2. The left graph shows a typical absorption curve for our 6.0 nm particles. The sharp absorption peak near wavelength $\lambda = 1640$ nm indicates that the energy bands have become nearly discreet due to the quantum confinement of the electrons and holes, in contrast to the continuous bands of bulk PbSe. The right side of Figure 2 shows the absorbance versus wavelength for all the sizes we obtained. The curves were shifted upwards sequentially to indicate larger particle sizes. The bottom curve corresponds to particles of size ∼3.5 nm while the top curve represents particles of size at least 10 nm. It is clear that the absorption peak shifts to shorter wavelength when the particle size is reduced.

In addition to the translational ordering from the hexagonal close packed assembly, the as synthesized samples also showed some directional ordering, that is, partial alignment of the crystallographic axes of the individual nanoparticles. The left graph of Figure 3 is TEM image showing partial directional ordering. Some of the darker particles can be seen to have finer patterns, which are aligned ∼45° to the horizontal line of the graph. The left side of Figure 3 is the electron diffraction ring pattern. In fact, the pattern is a hybrid of rings and six-fold dots, which means the film is between totally randomly aligned polycrystalline and totally aligned single crystalline. TEM also revealed that the inter-particle distance was 0.7–1.2 nm. After annealing, all the samples showed better directional ordering. When the annealing temperature was over 300 °C, the particles showed contact to each other and formed nanoarrays. Detailed TEM studies were published elsewhere [12].

The films obtained from controlled evaporation/precipitation method were not electrically conducting. In order for the films to be electrical conductive, capping organic agent that was left between particles must be removed. We tried annealing samples in vacuum, inert gas, diluted H_2 gas and oxygen. It turned out that at higher temperature, only diluted H_2 gas gave lower electrical resistance (R) and at lower temperature, vacuum

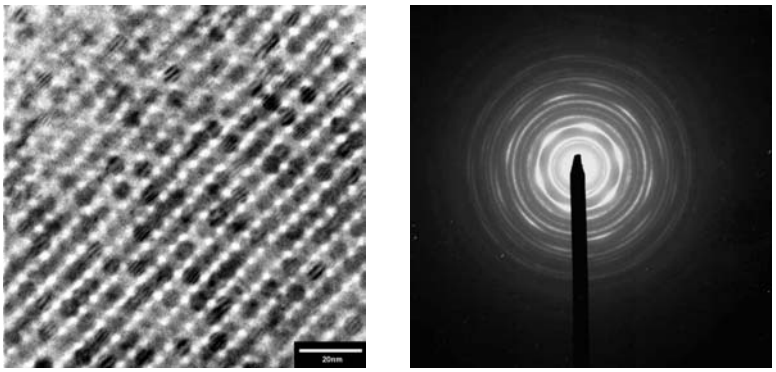

Figure 3: Partially ordered 6 nm PbSe particles from self-assembling. Left: TEM image showing that in addition to self-assembly, some 6 nm particles are clearly directionally ordered. Right: electron diffraction ring pattern indicating partial directional ordering.

and diluted H_2 gas were similar. Figure 4 shows the transport properties of a film annealed under flowing H_2 (8% H_2 and 92% Ar) at 425 °C for one hour. The resistance, R, of the sample was around 12 kΩ near room temperature and went up to ∼100 kΩ near 80 K. The sample was stable in air for at least a few days. The left-hand graph of Figure 4 shows the logarithm of R with respect to inverse temperature. The curve does not show any well defined linear behavior throughout the entire temperature range. However, an estimation near room temperature gives the energy gap $E_g = 42.8$ meV. The right-hand graph of Figure 4 shows Seebeck coefficient (S) measured for this sample. The curve is largely linear versus T. The negative value of S showed that the sample was n-type semiconductor near room temperature. This is in contrast to typical bulk PbSe samples that were p-type [13]. Unuma *et al* had shown, though, it was possible to dope PbSe with excess Pb [13]. Briefly, the Pb_2SeO_5 impurities were formed and gave rise to excess Pb when reduced by H_2, resulting n-type semiconductor. Although their experiments showed Pb doping only when sintering temperature was above ∼1000 K, our nanocrystalline samples are expected to be able to be reduced at a much lower temperature.

Although the sample annealed at 425 °C showed relative high value of $|S|$ and low R, essentially we destroyed the nanoparticles in such a high temperature. We had shown that the nanoparticles started to transform into nanoarrays at ∼300 °C. Further study showed that the organic species between the nanoparticles started to decompose at 240∼250 °C. Therefore, the samples were annealed at 250 °C in vacuum for 12 hours. As a result, the capping agent started to decompose and the sample surface was covered by a layer of residue. In such a case, attaching the electrical leads afterwards did not give any measurable electrical continuity. Eventually, we put the silver epoxy onto the sample before annealing. After annealing, the silver epoxy was covered by a layer of black residue and can be scratched away using a razor blade. Copper wires and other thermocouple wires were then attached to the sample using silver epoxy and baked in vacuum oven at 140 °C for about 30 minutes. The sample thus annealed had resistance below 8 kΩ but was not stable in air, because the protecting organic agent around the nanoparticles was gone. Figure 5

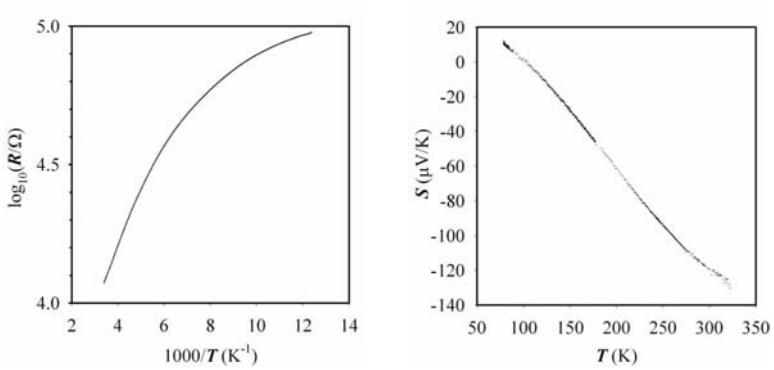

Figure 4: Transport properties of PbSe film annealed at 425 °C under flowing diluted H_2. Left: resistance in logarithm scale versus inverse of temperature showing $E_g = 42.8$ meV at room temperature. Right: negative S at room temperature indicates electron conduction.

shows $\log_{10}R$ versus $1000/T$ and S versus T. The sample showed a linear dependence in the temperature range of 265 K to 320 K with energy gap $E_1 = 35.7$ meV. A second linear region is observed between 130 K and 260 K with an energy gap of $E_2 = 15.5$ meV. These two values are smaller than the already small value of $E_g = 42.8$ meV obtained for the sample annealed at 425 °C. At this stage, we cannot conclude whether they are intrinsic features from nanoparticles or simply impurity energy levels. The thermoelectric power S was positive near room temperature, indicating p-type behavior, and was more or less linear versus T. S at room temperature matches well with the value of pure bulk PbSe reported by Unuma *et al* [13]. The value of S for our nanoparticle film is too low to be useful for thermoelectric applications at these temperatures unless the thermal conductivity (κ) is reduced due to scattering from the nanoparticle interfaces, which might be expected. However, these materials might be potentially useful at higher temperatures.

CONCLUSIONS

We have chemically synthesized nearly monodisperse colloids of highly-crystalline PbSe nanoparticles. The structural and optical properties of these nanoparticles were investigated. Nanoparticles with 6.0 nm average diameter were assembled into highly-ordered hexagonal close packed assembly over an area of at least 0.3×0.4 μm. The optical absorption of the colloids shows a series of absorption peaks which shift to shorter wavelengths with decreasing particle size, characteristic of semiconducting nanoparticle materials. We have also formed films of ordered nanoparticle assemblies and studied the electrical transport properties of these films. Thermoelectric transport properties of samples annealed at different temperatures were compared. We observed both n-type and p-type semiconducting behavior for differently annealed samples. For the first time, we were able to obtain electrically conductive PbSe films from nanoparticle colloids in which some of the nanometer-scale structure is preserved.

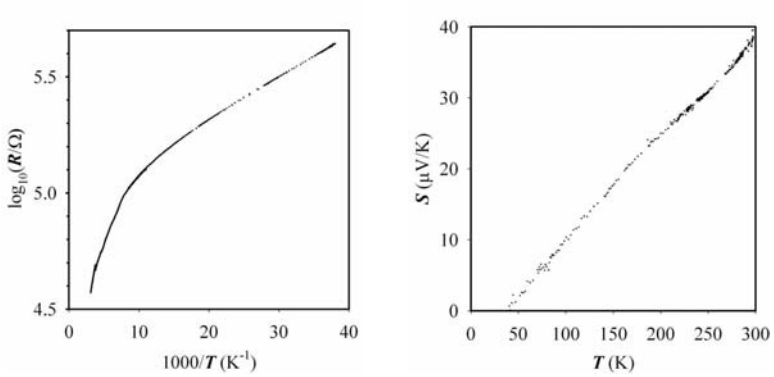

Figure 5: Transport properties of PbSe film annealed at 250 °C under vacuum. Left: resistance in logarithm scale versus inverse of temperature showing $E_g = 35.7$ meV at room temperature. Right: positive S at room temperature indicating hole as the major carrier.

ACKNOWLEDGMENTS

This work is supported by research grant DAAD19-99-1-0001 from the Army Research Office.

REFERENCES

[1] V. D. Das and K. S. Bhat, J. Mater. Sci. Mater. Electron. **1**, 169 (1990).
[2] G. A. Slack, *Thermoelectric Handbook*, CRC Press, Boca Raton, FL, 1995.
[3] T. Koga, T. C. Harman, S. B. Cronin, and M. S. Dresselhaus, Phys. Rev. B **47**, 14286 (1999).
[4] R. Venkatasubramanian, E. Silvola, T. Colpitts, and B. O'Quinn, Nature **413**, 597 (2001).
[5] L. D. Hicks and M. S. Dresselhaus, Phys. Rev. B **47**, 12727 (1993).
[6] C. B. Murray, C. R. Kagan, and M. G. Bawendi, Annu. Rev. Mater. Sci. **30**, 545 (2000).
[7] C. B. Murray, C. R. Kagan, and M. G. Bawendi, Science **270**, 1335 (1995).
[8] J. Fang, K. L. Stokes, W. L. Zhou, W. Wang, and J. Lin, Chem. Comm. **187**, 1872 (2001).
[9] F. Chen, J. C. Cooley, W. L. Hults, and J. L. Smith, Rev. Sci. Instr. **72**, 4201 (2001).
[10] R. B. Roberts, Philos. Mag. **36**, 91 (1977).
[11] F. Chen, K. L. Stokes, and R. Funahashi, (unpublished).
[12] W. L. Zhou, J. Wiemann, K. L. Stokes, and C. J. O'Connor, J. Microscopy and Microanalysis **7**, 314 (2001).
[13] H. Unuma, N. Shigetsuka, M. Takahashi, and K. Masui, J. Mater. Sci. Lett. **17**, 1055 (1998).